JOURNAL OF AIRCRAFT
Vol. 46, No. 1, January–February 2009

Aerodynamic Design of a Supersonic Inlet with a Parametric Bump

Sang Dug Kim*
Daegu University, Daegu 712-714, Republic of Korea

DOI: 10.2514/1.37416

Numerical investigations were performed with an external-compression inlet with a three-dimensional bump at Mach 2 to scrutinize the geometrical effects of the bump in controlling the interaction of a shock wave with a boundary layer. The inlet was designed for two oblique shock waves and a terminal normal shock wave followed by a subsonic diffuser, with a circular cross section throughout. The bump-type inlet that replaced the aft ramp of the conventional ramp-type inlet was optimized with respect to the inlet performance parameters as well as compared with the conventional ramp-type inlet. The current numerical simulations showed that a bump-type inlet can provide an improvement in the total pressure recovery downstream of the shock wave/boundary layer interaction over a conventional ramp-type inlet.

Nomenclature

A	=	sonic speed
D	=	characteristic length
D_o	=	exit diameter of inlet diffuser
H	=	height
h_o	=	nondimensional height of the bump
M	=	Mach number
L	=	length
l_o	=	nondimensional length of the bump
p	=	pressure
X	=	axis in a streamwise direction
Y	=	axis in a normal direction
y_n	=	normal distance from the wall surface
Z	=	axis in a spanwise direction

Subscripts

avg	=	mass-weighted average
o	=	inflow property
t	=	total property
∞	=	freestream value

I. Introduction

THE challenge of developing a novel propulsion system for high-speed aircraft has been an important research topic for the past half century. A critical component of such a propulsion system is the inlet, which must provide a homogeneous, low-speed, high-pressure airflow to the compressor face of an engine over a wide range of speeds, altitudes, and maneuvering conditions. High-speed aircraft generally require more complicated compression systems such as a series of movable compression ramps, porous walls, and slots controlled by sophisticated software and complex mechanical systems [1]. In a high-speed supersonic aircraft configuration (e.g., $M_\infty = 2$–5), a compression system produces a series of oblique shock waves, followed by a terminal normal shock wave and an adverse pressure gradient. The interaction of the shock wave with a turbulent boundary layer yields rapid thickening and separation of the boundary layer. Therefore, inlet designs for high-speed aircraft must eliminate the thick boundary layer which contains low-energy air that flows near the wall surface of the fuselage and inlet diffuser. Supersonic aircraft have dealt with this boundary layer phenomenon by redirecting the airflow using configurations such as a diverter of a gap between the fuselage and the upper lip of the inlet or the combinations of splitter plates and bleed systems [2]. The bleeding flow, which may remove the thick boundary layer from the inside of the inlet diffuser, can consume a significant fraction of the ingested inlet mass flow, and the amount required increases as the Mach number increases [3–5].

The concept of a three-dimensional curved surface of a bump has been used to control the boundary layer in a supersonic inlet flow. Simon et al. [6] studied an external bump-type inlet with boundary layer bleeding, which yielded satisfactory operational stability over a range of Mach numbers from 1.5–2. In this study, a three-dimensional bump (Fig. 1) was installed on the second ramp of a conventional ramp-type inlet. The bump-type inlet is an external-compression inlet where the terminal shock wave exists ahead of the cowl lip in a subcritical supersonic condition. It is expected that the innovative features of a bump-type inlet will remove the boundary layer with the effectiveness nearing that of a conventional ramp-type inlet, but without the complex and heavy mechanical bleeding systems [2,7]. The three-dimensional shape of the bump must adjust the inlet flow to prevent the low-energy airflow from entering the inside of the inlet diffuser. Therefore, it is of interest to study the effect of the parametric aspects of the bump geometry on the performance measures for a supersonic inlet. The bump geometries were the length and height of the bump because these may be critical factors that can reduce the interaction between the shock waves and boundary layers, and enhance the inlet performance.

II. Numerical Method

A. Governing Equation

The numerical simulation provided a highly effective tool for designing the bump-type inlet by simulating the inlet flows and evaluating the performance measures. The present three-dimensional computational analysis of a supersonic inlet flow including oblique/normal shock waves was performed using a numerical method [8] that integrates the governing equations for structured grids with a second-order upwind implicit scheme [9] for the convection terms of the conservation equations. The flow was modeled using the Reynolds-averaged Navier–Stokes equations for a thermally and calorically perfect gas and employing the Boussinesq hypothesis for turbulence modeling. The shear stress transport (SST) turbulence model was selected to close the Reynolds-averaged conservation equations due to its superior performance and stability compared with other turbulence models for adverse pressure flows as

Received 5 March 2008; revision received 30 May 2008; accepted for publication 30 May 2008.

*Visiting Professor, School of Automotive, Industrial and Mechanical Engineering, 15 Naeri-ri, Gyeongsan-si, Gyeongsangbuk-do, Korea; sangkim1@daegu.ac.kr.

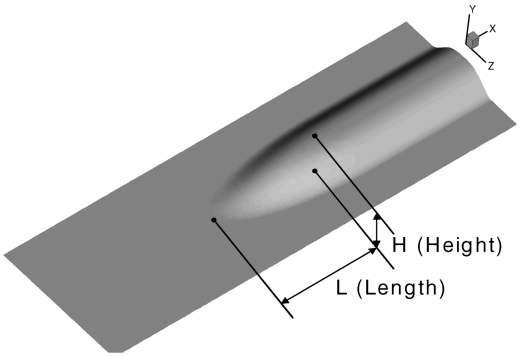

Fig. 1 Geometry of the three-dimensional bump installed on the aft ramp.

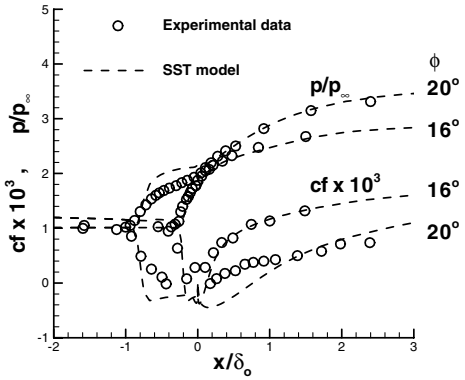

Fig. 2 Wall pressure and skin-friction coefficient distributions showing the comparison of the current numerical simulations with the experimental data of Settles et al. (1979) [12] for 16 and 20 deg ramps.

have been shown in previous investigations [10,11]. Figure 2 shows the applications for the supersonic compression corner cases, which imply a strong shock wave/boundary layer interaction. The free-stream Mach number was 2.85, and the two different ramp angles were 16 and 20 deg. The experiments of Settles et al. [12] dealt with the ramp placed on the bottom wall of a wind tunnel to generate the shock wave, which interferes with the turbulent boundary layer. The numerical simulations with the SST turbulence model used in this investigation produce a skin-friction coefficient recovery and wall pressure distribution downstream of the shock wave, which shows good agreement between the current simulation results and experiment data.

B. Grid System and Boundary Conditions

To obtain solutions to the conservation equations, boundary conditions are required for the computational domain. At the inflow boundary of the inlet, the incoming flow properties were prescribed by the freestream flow at Mach number of 2.0. At the outflow boundary, where the airflow exits the computational domain, the backpressure was specified to generate a normal shock wave in front of the cowl lip. No-slip and adiabatic wall conditions were imposed on the wall surfaces, and the spatial accuracy was of second order using the Roe flux-difference splitting upwind method. The simulations were conducted using an iterative method with local time stepping and multizone structured grids. The grid system was composed of eight blocks in which each has over 4×10^5 mesh points. The viscous mesh employed a first-grid point placement from the wall at y^+ less than unity. A stretching function was used to cluster grid points near the wall and shock locations. Convergence of the solutions was considered to be achieved when the L^2 norm of the maximum residual reached 10^{-4}.

III. Result and Discussion

The original ramp-type inlet model was tested in the experiment of Loth et al. [13] conducted in the NASA Langley Research Center

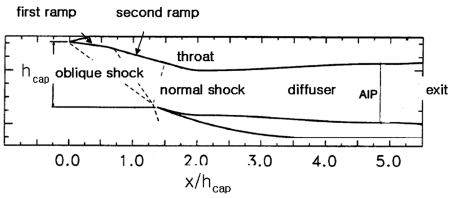

a) Schematic diagram of a conventional ramp-type inlet based on the experiment of Loth et al.[13]

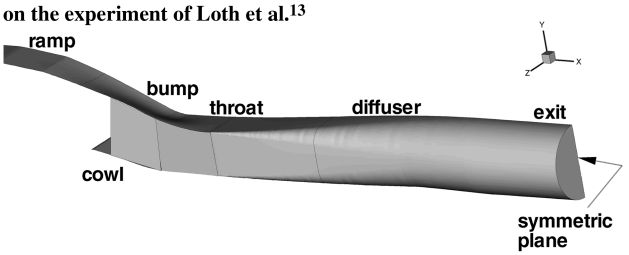

b) Three-dimensional bump-type inlet

Fig. 3 The geometries of supersonic inlets.

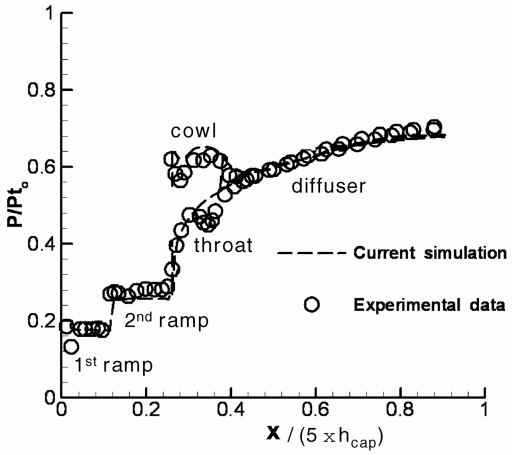

a) Wall pressure distributions

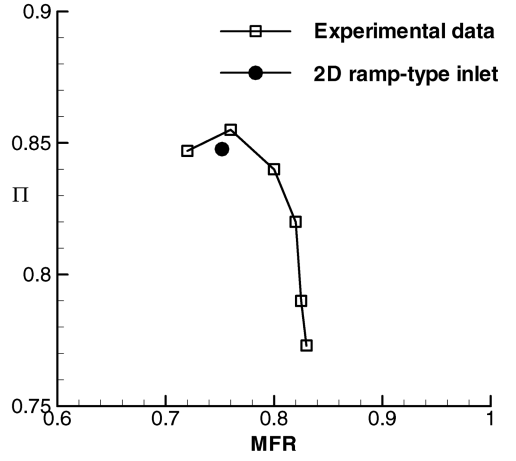

b) Total-pressure-recovery parameter

Fig. 4 Comparison of the current simulation with the experimental data of Loth et al. [13] for a ramp-type inlet with a rectangular cross-section diffuser.

Unitary Plan Wind Tunnel. The ramp-type inlet design was based loosely on an F-15 inlet (Fig. 3a), which had a low-expansion subsonic diffuser with a rectangular cross section throughout. The cross-sectional area was then expanded to a lower Mach number of approximately 0.45 at the aerodynamic interface plane (AIP), which relied on the one-dimensional analysis of the shock relationship and inviscid flow.

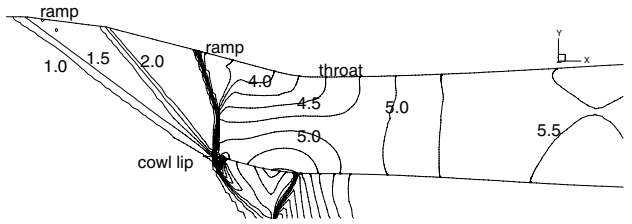

a) $h_o = 0.0$ (ramp type)

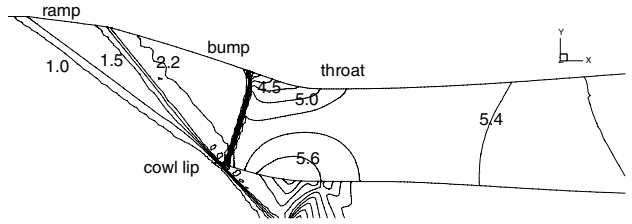

b) $h_o = 0.75$, $l_o = 0.75$

Fig. 5 Nondimensional static pressure contours on the symmetric plane of the ramp- and the bump-type inlets.

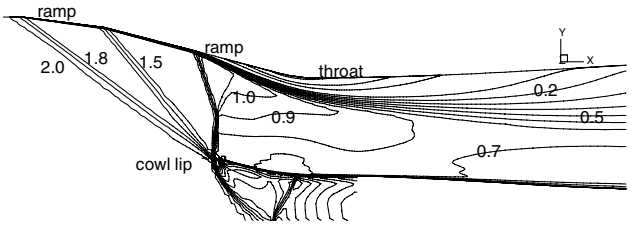

a) $h_o = 0.0$ (ramp type)

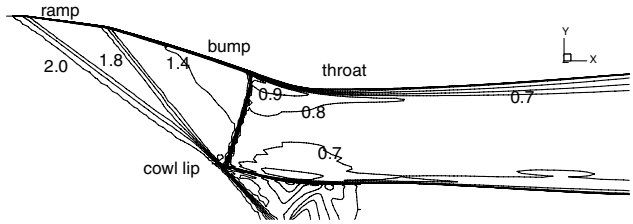

b) $h_o = 0.75$, $l_o = 0.75$

Fig. 6 Mach number contours on the symmetric plane of the ramp- and the bump-type inlets.

Figure 3b shows the half-geometry of a supersonic bump-type inlet in which the flowfield is assumed to be symmetric. The three-dimensional bump-type inlet consists of a ramp, bump, throat, cowl, and circular diffuser, which were based on the conventional ramp-type inlet of Loth et al. [13]. As shown in Fig. 3b, the aft ramp of the original ramp-type inlet was replaced by the three-dimensional bump. The ramp-type inlet of $h_o = 0$, however, adopted the original second ramp and the subsonic diffuser with a circular cross section throughout instead of the rectangular cross section used in the experiment.

Three-dimensional simulations with the SST turbulence model were conducted to evaluate the validation of the current numerical approach. The static pressure distribution, which was non-dimensionalized by the inflow stagnation pressure, was plotted along the longitudinal wall surface in Fig. 4a. Obvious sharp pressure increases appeared after the oblique and the normal shock waves in both the experiment and the current simulation. The predicted pressure rise eventually reached a level close to the theoretical inviscid pressure rise far downstream of the inlet throat. Figure 4b shows the comparison of the inlet performance between the experimental data [13] and the current two-dimensional ramp-type inlet simulation. The total-pressure-recovery parameter (Π) and the ratio of inlet mass flow (MFR) [13] were defined as follows:

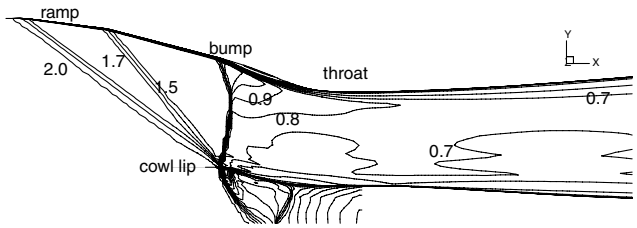

a) $h_o = 0.5$, $l_o = 0.25$

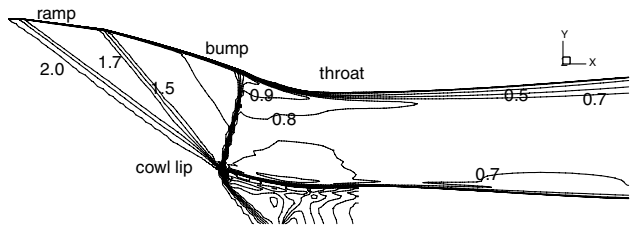

b) $h_o = 0.5$, $l_o = 0.5$

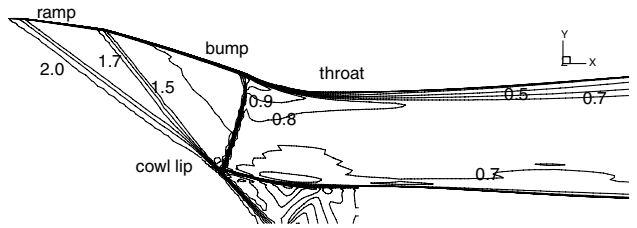

c) $h_o = 0.5$, $l_o = 0.75$

Fig. 7 Effect of the bump length on Mach number contours on the symmetric plane of bump-type inlets.

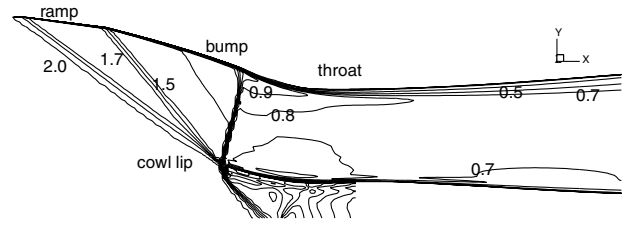

a) $h_o = 0.5$, $l_o = 0.5$

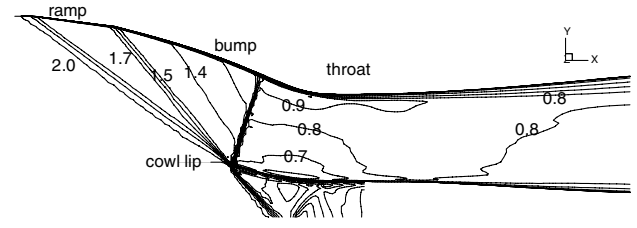

b) $h_o = 0.75$, $l_o = 0.5$

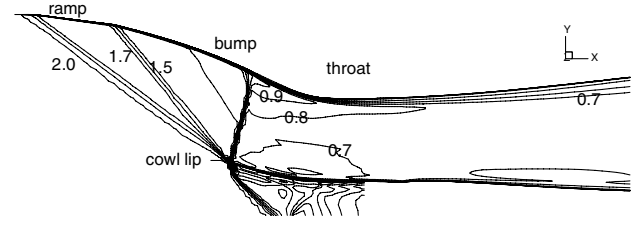

c) $h_o = 1.0$, $l_o = 0.5$

Fig. 8 Effect of the bump height on Mach number contours on the symmetric plane of bump-type inlets.

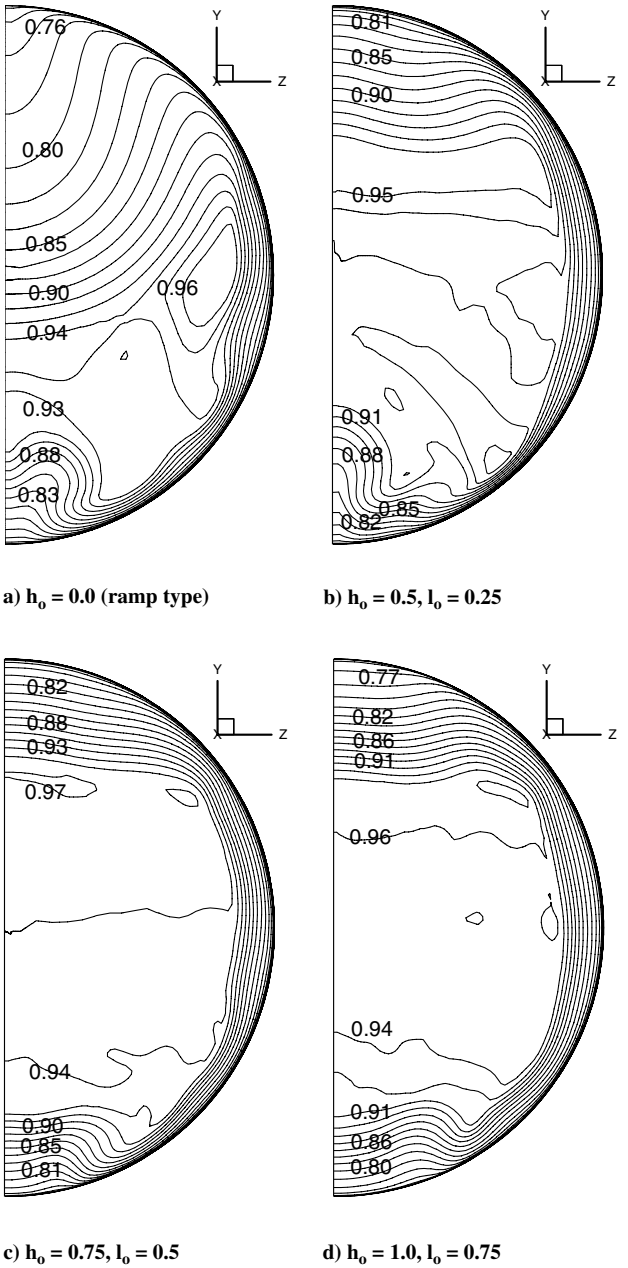

a) h_o = 0.0 (ramp type) **b) h_o = 0.5, l_o = 0.25**

c) h_o = 0.75, l_o = 0.5 **d) h_o = 1.0, l_o = 0.75**

Fig. 9 Nondimensional total-pressure contours at the AIP showing the comparison between a ramp-type inlet and three different bump-type inlets.

$$\Pi = \frac{P_{t,\text{avg}}}{P_{t,o}} \quad \text{and} \quad \text{MFR} = \frac{\text{mass flow through the AIP}}{\text{ideal capture mass flow}} \qquad (1)$$

This level of predictive fidelity was considered sufficient to have confidence in computationally evaluating the effect of the parametric aspects of the bump geometry on the inlet performance.

Figure 5 shows the nondimensional static pressure (p/p_∞) contours on the symmetric plane near the throat of the ramp- and the bump-type inlets. It includes a significant lambda-foot structure of the shock wave induced from the interaction with the boundary layer near the upper wall surface for $h_o = 0.0$, which is a ramp-type inlet (Fig. 5a). For $h_o = 0.75$, $l_o = 0.75$, the height is approximately 175% at the throat and the length is 75% of that of the aft ramp. This case produced a small region of shock wave/boundary layer interaction slightly upstream of the throat (Fig. 5b).

The ramp boundary layer was clearly thickened by passage through the strong shock wave/boundary layer interaction, which induces a slow flow recovery and a very thick boundary layer in the subsonic diffuser (Fig. 6a). The bleed system must consume a significant fraction of the inlet mass flow to remove this thick boundary layer. The bump-type inlet (Fig. 6b), however, showed that the flowfield rapidly recovered and retained a healthy boundary layer under the adverse pressure gradient in the subsonic diffuser. The bump-type inlet is then likely to eliminate the bleeding and the additional ducting systems, which can allow a significant reduction in weight for high-speed aircraft [5,13].

The numerical investigations revealed the critical factors and the direction for improvement in the aerodynamic design of a supersonic inlet. Figure 7 shows the effect of varying the bump length on the inlet flowfield on the symmetric plane near the throat. The short bump in the case of $l_o = 0.25$ yielded a relatively wider interaction region of the shock wave and boundary layer as compared with the other cases. Figure 8 shows that the oblique and the normal shock waves slightly in front of the cowl lip blended well with the bow shock wave, which was expelled from within the subsonic diffuser and expanded outward downstream of the cowl lip. The case of $h_o = 0.75$ had a smaller interaction region compared with the other cases, which indicated a need for an optimization procedure using the inlet performance measures.

The total-pressure distribution and development of the boundary layer in the supersonic inlet flowfield are important in assessing the inlet performance because their loss and nonhomogeneous distribution in the internal flow degrades engine performance and may severely reduce the lifetime of an aircraft. In particular, the shock wave/boundary layer interaction can produce significant total-pressure losses, boundary layer thickening, and flow nonuniformities at the compressor face of an engine. Figure 9 shows the comparison of the total-pressure contours at the AIP of the supersonic bump-type inlets, which revealed that the bump-type inlet might produce a higher recovery and wider uniform area of total pressure compared with the ramp-type inlet. Therefore, the three-dimensional bump has potential advantages to control the internal flow for high-quality airflows in supersonic inlets.

Figure 10 clearly shows the comparison of the nondimensional total-pressure profiles on the symmetric plane between the results of the experiment [13] and various bump-type inlet simulations. The experiment and the ramp-type inlet simulation show that the total-pressure profiles were severely distorted because the defected boundary layer was not recovered well under the adverse pressure gradient in the subsonic diffuser. The low-speed regions were, however, reduced significantly and the redeveloped profiles reached a high total-pressure recovery and were relatively uniform at the AIP in the bump-type inlets.

The optimization procedure was applied to determine the optimal value of the primary factors of the bump geometry as measured by maximizing the total-pressure recovery and minimizing the flow

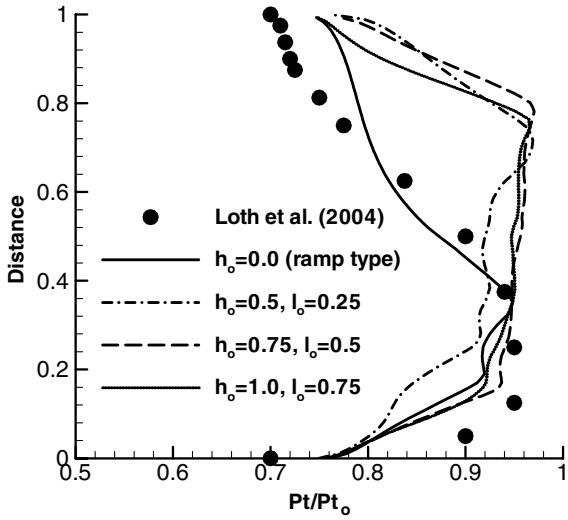

Fig. 10 Comparison of the nondimensional total-pressure profiles at the AIP on the symmetric plane between the experiment of Loth et al. [13] and various bump-type inlets.

distortion at the AIP. According to a precise investigation of the previous results, the geometrical factors of the bump were reduced to two critical factors that optimized the performance of the bump-type inlet. The influence and interaction of the critical factors, the length and height of the bump, were examined using the response surface methodology. The baseline value of each factor was centered, and its range was defined to create a quadratic response surface. The two-factor, three-level design required nine simulations and was suitable to explore the quadratic response surface and construct second-order polynomial models. The Fletcher–Reeves conjugate gradient method [14], which has advantages of using the conjugate search direction and the convergence in fewer iterations for truly quadratic problems, was used to obtain the mathematically optimum value.

Figure 11 plots the response surfaces of the total-pressure-recovery (Π) and the total-pressure-distortion (Δ) parameters over a range of design factors. The total-pressure-distortion parameter (Δ) was defined as

$$\Delta = \frac{(P_{t,\max} - P_{t,\min})}{P_{t,\text{avg}}} \tag{2}$$

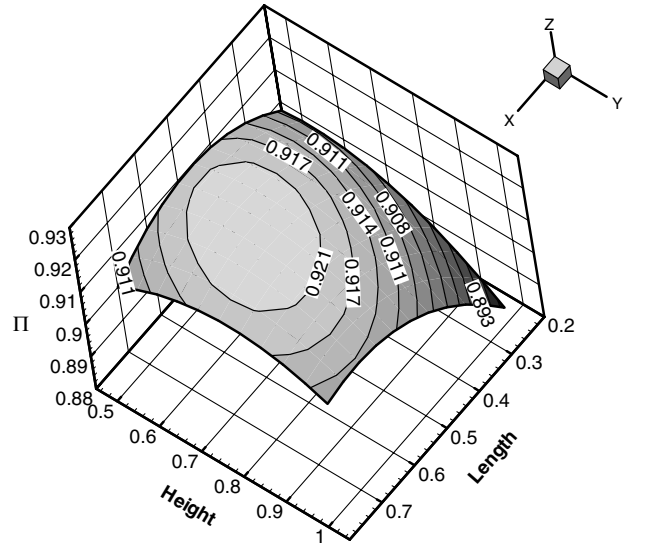

a) Total-pressure recovery (Π)

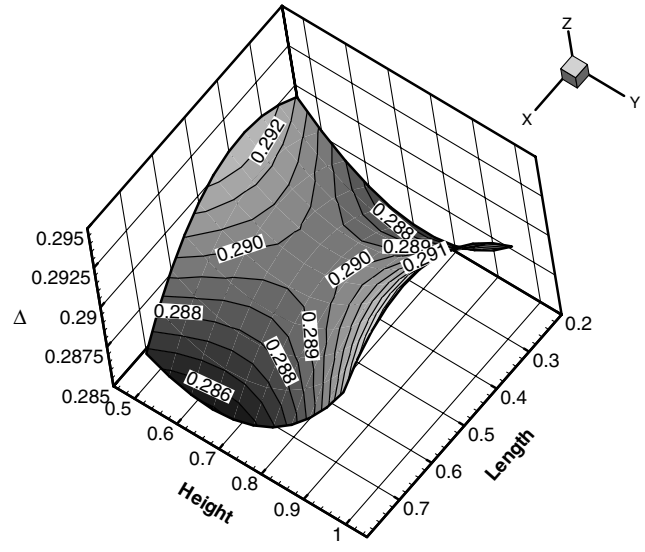

b) Total-pressure distortion (Δ)

Fig. 11 Performance of various bump-type inlets.

Because the static pressure is almost uniform at the AIP, the total-pressure distortion seems to be the flow distortion there. Figure 11 also shows that the optimized value of the total-pressure-recovery parameter (Π) is 0.923 at $(L, H) = (0.573, 0.700)$ from the quadratic equation, whereas the current simulation resulted in an optimum value of 0.925. The optimized value of the total-pressure-distortion parameter (Δ) is 0.285 at $(L, H) = (0.750, 0.646)$. The optimization procedures induced a significant increase in the bump-type inlet performance over the inlet with baseline geometry factors.

IV. Conclusions

Numerical investigations demonstrated a supersonic inlet flow at Mach 2 with shock wave/boundary layer interaction induced by a three-dimensional bump installed to replace the compression ramp used in conventional supersonic inlets. The current study showed that the geometrical features of the bump can play a critical role in reducing the total-pressure loss and maintaining a healthy boundary layer downstream of the shock wave/boundary layer interaction, which is able to produce an improvement in the total-pressure recovery and flow uniformity downstream of the subsonic diffuser. The bump-type inlet was optimized based on the design of experiments and the response surface method, as well as by comparisons with the conventional ramp-type inlet. The current numerical simulations and optimization showed that the bump-type inlet can provide an enhancement in the ability to control the shock wave/boundary layer interaction over a conventional ramp-type inlet.

Acknowledgment

This work was supported by the Korea Research Foundation Grant funded by the Korea Government (MOEHRD) (No. R08-2004-000-10556-0).

References

[1] Gridley, M. C., and Walker, S. H., *Advanced Aero-Engine Concepts and Controls*, CP-572, AGARD, 1996.

[2] Seddon, J., and Goldsmith, E. L., *Intake Aerodynamics*, Blackwell Science Ltd., London, 1999, pp. 336–340.

[3] Benson, J., and Miller, L. D., "Mach 5 Turbo-Ramjet Inlet Design and Performance," ISABE Conference, ISABE 91-7079, Nottingham, UK, September, Vol. 12, 1991, pp. 746–753.

[4] Nicolai, L. M., "Fundamental of Aircraft Design," METS Inc., San Jose, CA, 1975.

[5] Anderson, J., "Airframe/Propulsion Integration of Supersonic Vehicles," AIAA Paper 90-2151, July 1990.

[6] Simon, P. C., Brown, D. W., and Huff, R. G., "Performance of External-Compression Bump Inlet at Mach Number of 1.5 to 2.0," NACA RM-E56L19, National Advisory Committee for Aeronautics, WA, 1957.

[7] Tillotson, B. J., Loth, E., and Dutton, J. C., "Experimental Study of a Mach 3 Bump Compression Flowfield," *44th AIAA Aerospace Science Meeting and Exhibit*, AIAA, Reston, VA, 9–12 Jan. 2006.

[8] Kim, S. D., and Song, D. J., "The Numerical Study on the Supersonic Inlet Flow Field with a Bump," *Journal of Computational Fluids Engineering*, Vol. 10, No. 3, 2005, pp. 19–26.

[9] Hirsh, C., *Numerical Computation of Internal and External Flows*, Vol. 2, Wiley, New York, 1989, pp. 493–594.

[10] Kim, S. D., and Song, D. J., "Modified Shear-Stress Transport Turbulence Model for Supersonic Flows," *Journal of Aircraft*, Vol. 42, No. 5, 2005, pp. 1118–1125.

[11] Kim, S. D., Kwon, C. O., and Song, D. J., "Comparison of Turbulence Models in Shock-Wave/Boundary-Layer Interaction," *KSME International Journal*, Vol. 18, No. 1, 2004, pp. 153–166.

[12] Settles, G. S., Fitzpatrick, T. J., and Bogdonoff, S. M., "Detailed Study of Attached and Separated Compression Corner Flowfields in High Reynolds Number Supersonic Flow," *AIAA Journal*, Vol. 17, No. 6, 1979, pp. 579–585. doi:10.2514/3.61180

[13] Loth, E., Jaiman, R., Dutton, C., White, S., Roos, F., Mace, J., and Davis, D., "Mesoflap and Bleed Flow Control for a Mach 2 Inlet," AIAA Paper 2004-855, 5–8 Jan. 2004.

[14] Burgreen, G. W., and Baysal, O., "Aerodynamic Shape Optimization Using Preconditioned Conjugate Gradient Methods," *AIAA Journal*, Vol. 32, No. 11, 1994, pp. 2145–2152. doi:10.2514/3.12271